AD-A116 899 HOWARD UNIV WASHINGTON DC DEPT OF CHEMISTRY F/G 20/3
SURFACE RAMAN SCATTERING FROM EFFERVESCENT MAGNETIC PEROXYBORAT--ETC(U)
JUN 82 G E WALRAFEN, P N KRISHNAN N00014-80-C-0305
UNCLASSIFIED TR-11 NL

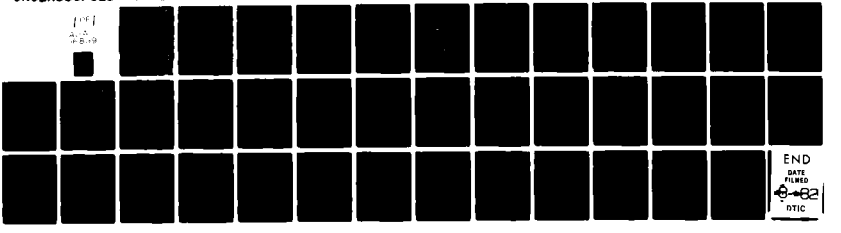

SECURITY CLASSIFICATION OF THIS PAGE *(When Data Entered)*

REPORT DOCUMENTATION PAGE		READ INSTRUCTIONS BEFORE COMPLETING FORM
1. REPORT NUMBER: 11	2. GOVT ACCESSION NO.: AD-A116899	3. RECIPIENT'S CATALOG NUMBER:
4. TITLE *(and Subtitle)*: Surface Raman Scattering From Effervescent Magnetic Peroxyborates		5. TYPE OF REPORT & PERIOD COVERED: Technical Report #11
		6. PERFORMING ORG. REPORT NUMBER:
7. AUTHOR(s): G.E. Walrafen, D.L. Griscom, P.N. Krishnan, R. Munro		8. CONTRACT OR GRANT NUMBER(s): N00014-80-C-0305
9. PERFORMING ORGANIZATION NAME AND ADDRESS: Department of Chemistry, Howard University, Washington, D.C. 20059		10. PROGRAM ELEMENT, PROJECT, TASK AREA & WORK UNIT NUMBERS: NR-051-733
11. CONTROLLING OFFICE NAME AND ADDRESS: Office of Naval Research, Department of the Navy, Arlington, Virginia 22217		12. REPORT DATE: June 30, 1982 13. NUMBER OF PAGES: 34
14. MONITORING AGENCY NAME & ADDRESS *(if different from Controlling Office)*		15. SECURITY CLASS. *(of this report)*: Unclassified 15a. DECLASSIFICATION/DOWNGRADING SCHEDULE

16. DISTRIBUTION STATEMENT *(of this Report)*

Approved for public release; reporduction is permitted for any purpose of the United States government distribution is unlimited.

17. DISTRIBUTION STATEMENT *(of the abstract entered in Block 20, if different from Report)*

Distribution of this document is unlimited

18. SUPPLEMENTARY NOTES

Prepared and accepted for publication in the Journal of Chemical Physics.

19. KEY WORDS *(Continue on reverse side if necessary and identify by block number)*

Raman Scattering, Magnetic Peroxyborates, Logistic Theory

20. ABSTRACT *(Continue on reverse side if necessary and identify by block number)*

Surface Raman scattering using a spinning technique was investigated for solid $NaBO_3.4H_2O$ and $NaBO_3.H_2O$ as well as for electron bombarded peroxyborates heated for various times and at temperatures from 110-180° C, and for solid Na_2O_2 and BaO_2. The Raman spectra indicate that the breakdown of peroxy groups is accompanied by the formation of trapped molecular O_2. Quantitative Raman intensity data were also obtained as functions of heating time at 115°C for the 1556cm^{-1} line from O_2 and for the 890 and 705cm^{-1} lines whose intensities scale with the peroxy concentration. These intensity data were treated by logistics theory,

DD FORM 1 JAN 73 1473 EDITION OF 1 NOV 65 IS OBSOLETE
S/N 0102-014-6601

ABSTRACT CONTINUED

SECURITY CLASSIFICATION OF THIS PAGE *(When Data Entered)*

REPORT DOCUMENTATION PAGE		READ INSTRUCTIONS BEFORE COMPLETING FORM
1. REPORT NUMBER	2. GOVT ACCESSION NO.	3. RECIPIENT'S CATALOG NUMBER
4. TITLE *(and Subtitle)*		5. TYPE OF REPORT & PERIOD COVERED
		6. PERFORMING ORG. REPORT NUMBER
7. AUTHOR*(s)*		8. CONTRACT OR GRANT NUMBER*(s)*
9. PERFORMING ORGANIZATION NAME AND ADDRESS		10. PROGRAM ELEMENT, PROJECT, TASK AREA & WORK UNIT NUMBERS
11. CONTROLLING OFFICE NAME AND ADDRESS		12. REPORT DATE
		13. NUMBER OF PAGES
14. MONITORING AGENCY NAME & ADDRESS*(if different from Controlling Office)*		15. SECURITY CLASS. *(of this report)*
		15a. DECLASSIFICATION/DOWNGRADING SCHEDULE
16. DISTRIBUTION STATEMENT *(of this Report)*		
17. DISTRIBUTION STATEMENT *(of the abstract entered in Block 20, if different from Report)*		
18. SUPPLEMENTARY NOTES		
19. KEY WORDS *(Continue on reverse side if necessary and identify by block number)*		

20. ABSTRACT *(Continue on reverse side if necessary and identify by block number)*

and they were found to be consistent with a second-order auto-catalyzed forward reaction dependent on the product of the peroxy and O_2 concentrations, plus a first-order reverse reaction dependent only on the O_2 concentration.

DD FORM 1 JAN 73 1473 EDITION OF 1 NOV 65 IS OBSOLETE
S/N 0102-014-6601 |

SECURITY CLASSIFICATION OF THIS PAGE *(When Data Entered)*

"SURFACE RAMAN SCATTERING FROM EFFERVESCENT MAGNETIC PEROXYBORATES"

by

G. E. Walrafen and P. N. Krishnan*
Chemistry Department
Howard University
Washington, D. C. 20059

and

D. L. Griscom
U. S. Naval Research Laboratory
Code 644 3
Washington, D. C. 20375

and

R. Munro
Center for Materials Science
National Bureau of Standards
Washington, D. C. 20234

*Visiting from Coppin State College,
Baltimore, Maryland 21216

ABSTRACT

Surface Raman scattering using a spinning technique was investigated for solid $NaBO_3 \cdot 4H_2O$ and $NaBO_3 \cdot H_2O$, as well as for electron bombarded peroxyborates, for peroxyborates heated for various times and at temperatures from 110-180° C, and for solid Na_2O_2 and BaO_2. The Raman spectra indicate that the breakdown of peroxy groups is accompanied by the formation of trapped molecular O_2. Quantitative Raman intensity data were also obtained as functions of heating time at 115° C for the 1556 cm^{-1} line from O_2 and for the 890 and 705 cm^{-1} lines whose intensities scale with the peroxy concentration. These intensity data were treated by logistics theory, and they were found to be consistent with a second-order auto-catalyzed forward reaction dependent on the product of the peroxy and O_2 concentrations, plus a first-order reverse reaction dependent only on the O_2 concentration.

INTRODUCTION

Peroxyborates[1] are borate compounds containing peroxy linkages. They may be prepared as crystalline hydrates by evaporating the aqueous metaborate[1] solutions with hydrogen peroxide. The structure of the peroxyborate anion in the tetrahydrate,[2] $NaBO_3 \cdot 4H_2O$, involves the tetrahedral dimeric structure determined by Hansson,[3] Fig. 1. A monohydrate,[2] $NaBO_3 \cdot H_2O$, can also be obtained by dehydration between 55-60°C according to the reversible reaction,

$$NaBO_3 \cdot 4H_2O \rightleftharpoons NaBO_3 \cdot H_2O + 3H_2O, \qquad (1)$$

during which the peroxyborate anion structure of Fig. 1 is thought to remain unchanged. Careful additional heating between 100-130°C yields an amorphous, slightly heterogeneous modification which releases up to 10 wt.% of gaseous oxygen upon dissolution in water,[4,5] and is highly paramagnetic. This modification is the effervescent Magnetic Peroxy Borate (EMPB)[5] studied here.

Edwards et al.[5] have presented various types of data leading to a reasonably complete structural description of EMPB's. Mass spectra from samples in which both oxygen atoms in a peroxy linkage were labelled with ^{18}O demonstrated (1) that the oxygen released in water (active oxygen) originates exclusively from the peroxy linkages in the parent crystalline forms, and (2) that the breaking and reforming of peroxy

(1)

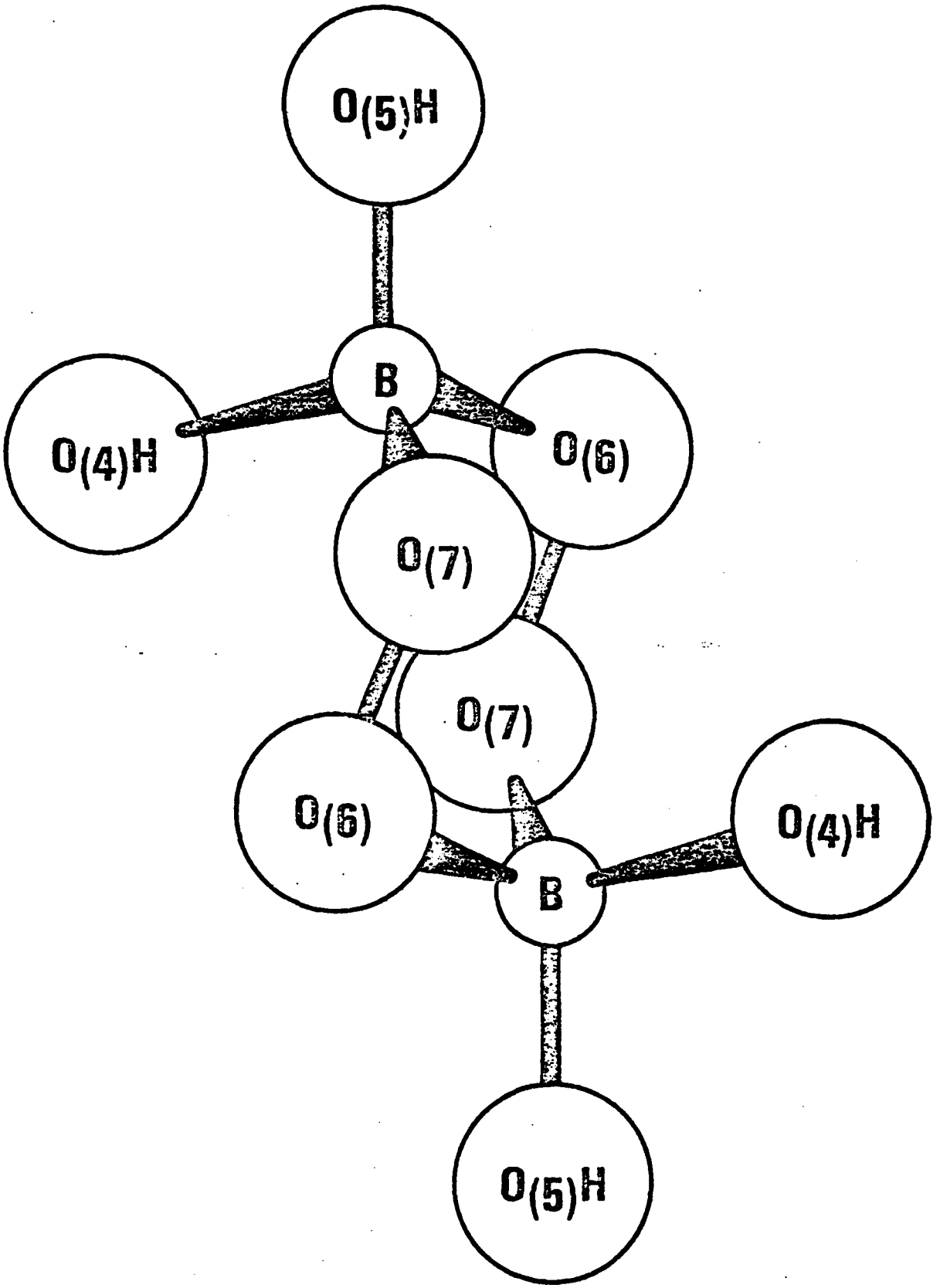

Caption

Figure 1. Structure of the peroxyborate anion, $[B_2(O_2)_2(OH)_4]^{2-}$. Bond distances are B-O_4, 1.54Å; B-O_5, 1.44Å; B-O_6, 1.52Å; B-O_7, 1.42Å; O_6-O_7; 1.47Å. Figure and data from Hansson.[3]

linkages is directly involved in forming the amorphous material. Infrared and x-ray diffraction studies also demonstrated that the most extensively reacted preparations still retain small amounts of the unreacted starting material ($NaBO_3 \cdot H_2O$), and that no new crystalline phase results. Further, the presence of unusually high paramagnetic spin concentrations (to 4.6x 10^{21} cm^{-3} assuming S=1/2, or to 1.7 x 10^{21} cm^{-3} for S=1) was revealed by static susceptibility measurements.

The spin concentrations from static susceptibility measurements exceeded the known impurity content by several orders of magnitude, and thus paramagnetic states were ascribed to various oxyanions. Two relatively weak overlapping components in the ESR spectra were reliably attributed to O_2^- and O_3^-.[6] Moreover, the presence of O_2 or oxyanions requires changes in the boron coordination from 4 to 3. ^{11}B - NMR spectra were consistent with coordination changes of up to ~15% for the total B in extensively reacted EMPB preparations. Both the static susceptibility and the overall ESR intensity were shown to correlate nearly linearly with the wt.% active oxygen. However, the magnetic susceptibility indicated total paramagnetic spin concentrations more than three times those estimated by ESR. This and other considerations led to the suggestion [5,6] of interstitial O_2 molecules having S=1 spin states. Such molecules would contribute to the susceptibility, but if not free to rotate, they would escape ESR detection, because the zero field splitting substantially exceeds the energies of the microwave quanta involved in the experiment.[7]

Raman methods were used in this work because the infrared method is insensitive to O_2,[8] as well as the in-phase stretching

vibrations of (two) peroxy groups. $NaBO_3 \cdot 4H_2O$, $NaBO_3 \cdot H_2O$ and EMPB preparations were examined and found to give intense Raman spectra when sample spinning was employed.(9) Further, a sharp Raman line at 1556±2 cm^{-1} was readily observed for EMPB samples heated for 2 h or more at 115° C (but not for $NaBO_3 \cdot H_2O$ samples that were electron bombarded but not heated). The 1556 cm^{-1} frequency is identical to that reported for the O-O stretching vibration of gaseous O_2.(10) thus clearly indicating the presence of O_2 trapped in heated EMPB's. Raman spectra were also obtained for solid BaO_2 and Na_2O_2. A weak Raman line was observed at 1136 cm^{-1} for Na_2O_2 in reasonable agreement with the O-O stretching vibration of O_2^-.(11) EMPB samples both heated and electron bombarded were examined for O_2^- by Raman methods, but no intensity near 1136 cm^{-1} was observed that could be directly related to the O_2^- concentrations involved. The ESR resonance identified in Ref. (6) as the Z-resonance, most closely approximates the resonance from Na_2O_2 due to O_2^-.(6) The concentration corresponding to the Z-resonance in the EMPB samples studied here(6) ranged from about 4×10^{18} cm^{-3} to 1×10^{20} cm^{-3}, i.e., too low for Raman detection where interfering vibrations are involved.

Quantitative Raman intensity measurements were also made of the 1556 cm^{-1} O_2 intensity, and also of two lines at 705 and 890 cm^{-1}, whose intensities scale with the peroxy concentrations, as functions of heating time at 115° C. These and other Raman data are now described.

EXPERIMENTAL

Raman spectra were obtained by a sample spinning method.(9) Intensity data were obtained by using Na_2SO_4 as an internal Raman standard. An EMPB mixture containing a constant percentage by weight of Na_2SO_4 was prepared. The Na_2SO_4 was evenly dispersed in the EMPB mixture by thorough grinding. The corresponding Raman spectra contained contributions both from the EMPB and from the SO_4^{2-} ion. Because the SO_4^{2-} concentration was constant, the intensities from the EMPB's heated for various times could be related quantitatively to the, $\nu_1 A_1$, Raman intensity of SO_4^{2-} at 990 cm^{-1}.

The Raman spectra were obtained with an Instrument S.A. HG-2S holographic grating double monochromator. Radiation at 488.0 and 514.5nm from an argon ion laser operated at power levels near 1 W was used for excitation. Slit-widths used for the EMPB's corresponded to ~5 cm^{-1} and to 2 cm^{-1} for the BaO_2 and Na_2O_2 samples. The detection and recording apparatus have been described previously.(9)

SURVEY RAMAN SPECTRA

A series of survey Raman spectra was obtained prior to obtaining Raman intensity data. This series involved spectra from: (1) $NaBO_3 \cdot 4H_2O$, (2) $NaBO_3 \cdot H_2O$, (3) $NaBO_3 \cdot H_2O$ subjected to low electron dosage 5.6×10^{14} electrons/cm^2, (4) $NaBO_3 \cdot H_2O$ heated at 110°C and then subjected to high dose 1.3×10^{16} electons/cm^2 electron irradition [(1)-(4), shown in Fig. 2], (5) $NaBO_3 \cdot H_2O$ heated for various times and at various temperatures, 2-4 h at 125°C, 4-14 h at 155°C, and 5-6 h at 180°C, and (6) Na_2O_2, and (7) BaO_2 [(6) and (7), shown in Fig. (3)].

The Raman spectra from $NaBO_3 \cdot 4H_2O$ and $NaBO_3 \cdot H_2O$, Fig. 2, (d) and (c), are similar in the vibrational region from 0-1800 cm^{-1}. Apart from some small differences below 600 cm^{-1}, e.g., intensity variations and half-width changes, the main spectral differences occur between 600-1000 cm^{-1}. Here, Raman lines from $NaBO_3 \cdot 4H_2O$ occur at 710, 900, and 970 cm^{-1}, whereas lines from $NaBO_3 \cdot H_2O$ occur at 705, 890, and 960 cm^{-1}. Also ratios of the 705-710 cm^{-1} intensity to the intensities at 890-900 cm^{-1} or 960-970 cm^{-1}, Fig. 2, are about twice as large for $NaBO_3 \cdot H_2O$ as for $NaBO_3 \cdot 4H_2O$. However, the gross features of the line patterns observed from $NaBO_3 \cdot H_2O$ or $NaBO_3 \cdot 4H_2O$ seem too similar to suggest any major change in the peroxyborate anion structure with changing hydration, Fig. 1.

The Raman spectra from $NaBO_3 \cdot H_2O$ subjected to low-dose electron irradiation, Fig. 2 (b), are also not grossly different from those of untreated $NaBO_3 \cdot H_2O$. The most conspicuous difference involves a change

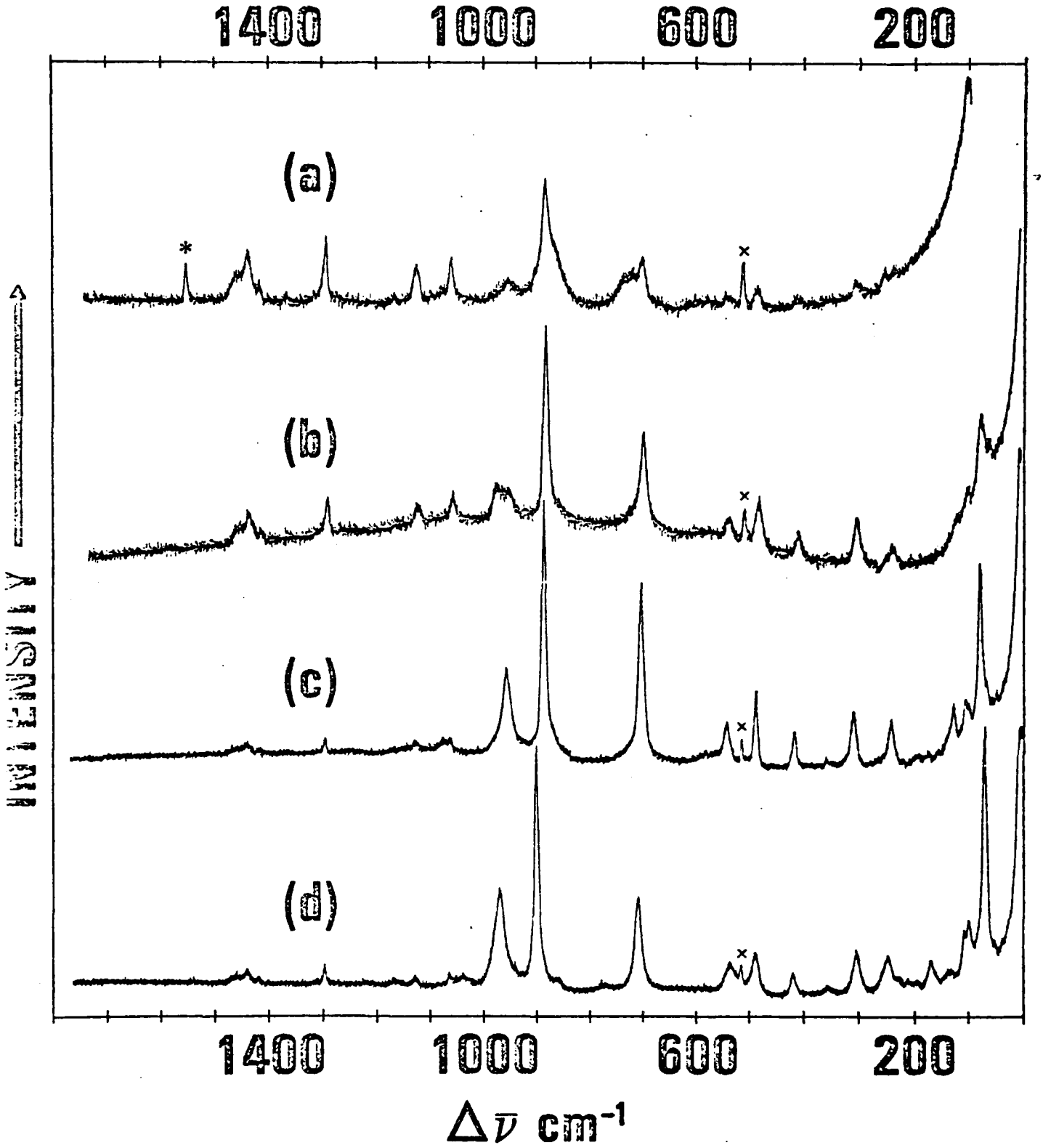

(2)

Caption

Figure 2. Raman spectra from solid EMPB's (a) heated at 110°C and irradiated with 1.3×10^{16} electrons/cm^2, (b) 5.6×10^{14} electrons/cm^2 but no heating (c) $NaBO_3 \cdot H_2O$, and (d) $NaBO_3 \cdot 4H_2O$. Spectra were obtained with 514.5 nm excitation using slit widths of 5-8 cm^{-1} and laser power levels from 0.6 -1.0 W. The effective gains (intensity scaling factors) for (d), (c), (b), and (a) are, respectively, 1, 0.7, 2 and 4. The sharp Raman line from trapped molecular O_2 at 1556 cm^{-1} is indicated by (*). An intense plasma line from A_F^+ near 520 cm^{-1} is indicated by (X).

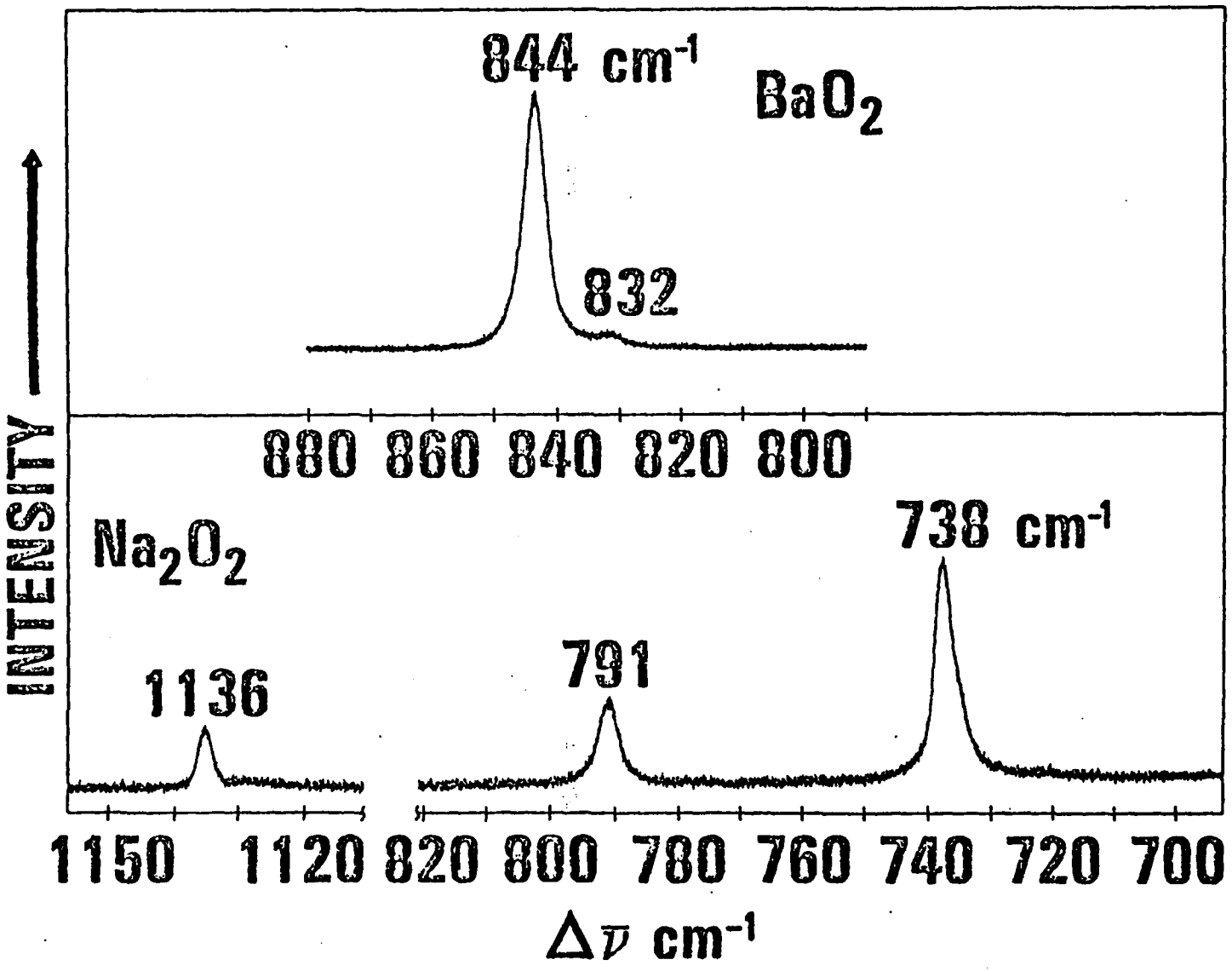
844 cm⁻¹
BaO2
832
880 860 840 820 800
INTENSITY
Na2O2
738 cm⁻¹
1136
791
1150 1120 820 800 780 760 740 720 700
Δν cm⁻¹

Caption

Figure 3. Raman spectra from solid Na_2O_2 and BaO_2. The spectra were obtained with 488.0 nm excitation at a power level of 1 W using a slit width of 2 cm^{-1} and a scanning rate of 5 cm^{-1}/min. The gain in the lower spectrum from Na_2O_2 was increased by a factor of 3.33 to record the weak maximum due to O_2^- at 1136 cm^{-1}, see region to the left between about 1120-1150 cm^{-1}.

from a sharp line for $NaBO_3 \cdot H_2O$ at 960 cm^{-1}, to a weaker unresolved doublet having peaks near 955 and 975 cm^{-1} after the electron dose.

The Raman spectra from $NaBO_3 \cdot H_2O$ heated at 110°C, and then subjected to high-dose electron irradiation, Fig. 2(a), differ significantly from those of untreated $NaBO_3 \cdot H_2O$. The spectra show new features, e.g., at about 725-745 cm^{-1}, 865-890 cm^{-1}, and 1556 $\pm$ 2 cm^{-1}. The sharp line at 1556 cm^{-1} agrees with the 0-0 stretching vibration reported for gaseous O_2.(10) The broad new features near 725-740 and 865-890 cm^{-1} also are present in spectra corresponding to long heating times (no electron bombardment). Hence, they may refer to vibrations of groups remaining after the peroxy groups have reacted to form molecular O_2.

In Raman spectra from samples heated, for example, for 14 h at 155°C, the sharp features near 705 and 890 cm^{-1} are not observed, and the 1556 cm^{-1} peak height is the largest in the spectrum. Raman spectra from less rigorously treated samples, e.g., 2 h at 125°C fall between those from unheated and strongly heated samples. Such spectra suggest that the O_2 concentration increases as the concentration of the peroxy groups decreases. Further, comparisons with spectra from samples that were only electron bombarded suggest that heating may have the greater effect. Certainly, the 1556 cm^{-1} line is not seen from samples subjected to low-dose electron irradiation alone, whereas mild heating, 2 h at 115°C, readily produces it in the spectrum.

Raman spectra from Na_2O_2, Fig. 3 (b), reveal an intense asymmetric line at 738 cm^{-1} (with an unresolved low-frequency shoulder),

and two weaker lines at 791 and 1136 cm^{-1}. The intensity of the 1136 cm^{-1} line is roughly one-tenth that of the 738 cm^{-1} line. It is assigned to O_2^- in reasonable agreement with the previously reported value of 1145 cm^{-1}.[11] In contrast, the spectrum from solid BaO_2 does not display any line in the vicinity of 1136 cm^{-1}, Fig. 3(a). This spectrum yields an intense line at 844 cm^{-1} with a resolved foot near 832 cm^{-1}. The intense lines at 738 and 844 cm^{-1} are assigned to symmetric O-O stretching vibrations of O_2^{2-} in different environments. The electron irradiated samples corresponding to Figs. 2(b) and 2(a),[12] yield O_2^- concentrations as determined by ESR measurements of $\sim 4 \times 10^{18}$ cm^{-3} and $\sim 1 \times 10^{20}$ cm^{-3}, resp.[6] Both samples also yield a weak Raman line near 1124 cm^{-1}. However, this line cannot reliably be related to O_2^-, Fig. 3, because lines at similar frequencies were seen for untreated $NaBO_3 \cdot 4H_2O$ and $NaBO_3 \cdot H_2O$, and also the O_2^- concentrations determined by ESR[6] are too low for Raman detection.

Finally, the O_2 Raman line at 1556 cm^{-1} was observed from samples heated 14 h at 155° C, and, with diminished intensity, from samples heated 6 h at 180° C. Thus, it seems reasonable to conclude that both the final decomposed amorphous material, as well as the partially amorphized EMPB, effectively trap O_2 molecules.

Quantitative Raman Intensity Data

Raman intensity data for the 1556 cm^{-1} line of O_2, and for the 890 and 705 cm^{-1} lines, the former of which is directly assigned to peroxy groups, are shown as functions of heating time in hours, t, at 115° C in Fig. 4 (a)-(c). The intensity, $I_{1556}(t)$, Fig. 4(a), is seen to increase in a sigmoidal fashion from about zero at t=0, to a constant value at t>6 h. Simultaneously, the intensities $I_{890}(t)$ and $I_{705}(t)$, Fig. 4(b) decrease and reach constant, but nonzero, values for t>6 h. The 890 and 705 cm^{-1} intensities also behave in the same way with time, as is evident from Fig. 4(b), and particularly from Fig. 4(c) as shown by the constancy of the intensity ratios. This constancy, 1.6±0.1, indicates that the two vibrations involved refer to a common structural unit, e.g., $\left[B_2(O_2)_2(OH)_4\right]^{2-}$.

The intensity data shown in Fig. 4(a) and (b) are characteristic of those arising from logistics theory[13], and were treated according to that theory, see Appendix I.

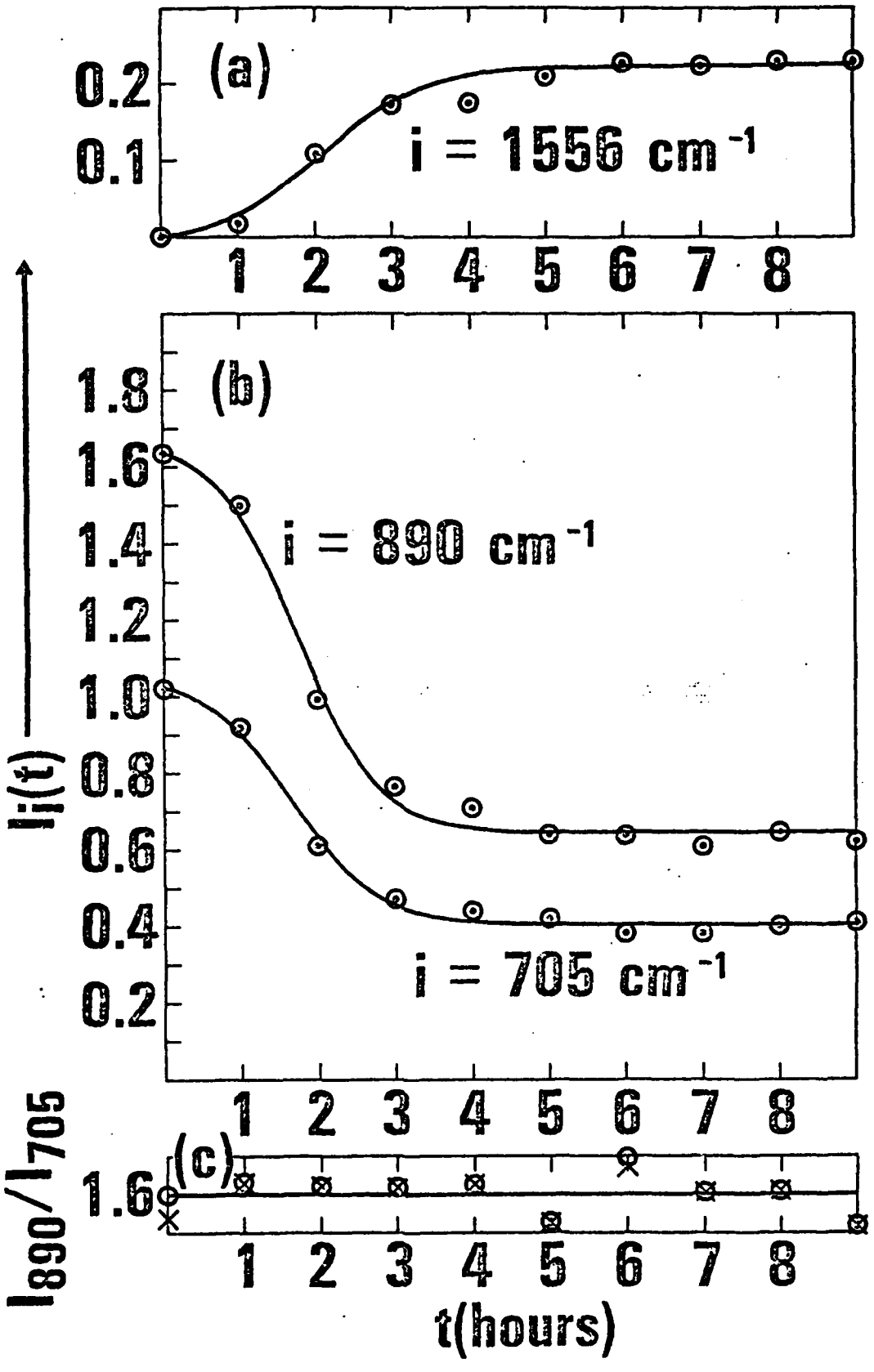
(a)
i = 1556 cm⁻¹
0.2
0.1
1 2 3 4 5 6 7 8
(b)
i = 890 cm⁻¹
i = 705 cm⁻¹
1.8
1.6
1.4
1.2
1.0
0.8
0.6
0.4
0.2
Ii(t)
1 2 3 4 5 6 7 8
(c)
I890/I705
1.6
1 2 3 4 5 6 7 8
t(hours)

Caption

Figure 4. Quantitative Raman intensities, $I_i(t)$, versus heating time in hours at 115°C for (sodium) EMPB samples. The intensities refer to peak heights corrected for overlap of neighboring components relative to the peak height from a SO_4^{2-} internal standard at 990 cm^{-1}. The intensity data, $I_i(t)$, were fitted by least squares using logistics theory and the quantity $L_i(t)$ defined in Appendix I. In (a), $I_i(t) = L_i(t)$. However, in (b), $I_i(t) = I_i(0) - L_i(t)$. $I_{705}(0) = 1.021$, and $I_{890}(0) = 1.634$.

Printer note: $I_i(t)$

$I_{1i}(t)$

The differential equation from logistics theory for the case where $\Phi(t) = \frac{-a}{k}$ is readily shown to be identical to the equation corresponding to second order auto-catalyzed reactions (see Appendix I.) For the auto-catalyzed reaction A→B, the rate law is,(14)

$$-d[A]/dt = k_2 [A] [B]. \qquad (2)$$

But when $y=[A]$, $k_2=\Phi(t) = \frac{-a}{k}$, and $k= [A] + [B]$ (mass conservation), Appendix I, eqn. (2) is identical to eqn. (7). (Note that $y=[A] \propto I_{705}$ or I_{890}, $[B] = (k-y) \propto I_{1556}$, A = peroxy, B = O_2.)

Eqn. (2), however, requires that $[A]_\infty=0$, whereas Fig. 4 (b) indicates that I_{890} (∞) or I_{705} (∞) are nonzero. To resolve this difficulty consider that the correct rate equation for the present case is given by,

$$-d[A]/dt = k_2[A] [B] - k_1[B]. \qquad (3)$$

Eqn. (3) implies that $[A]_\infty \neq 0$ because A is replenished by a first order reverse reaction in B. In this case if $k_1=k_2[A]_\infty$, eqn. (3) takes the form,

$$-d[A]/dt = -d([A]-[A]_\infty)/dt = k_2([A]-[A]_\infty) [B]. \qquad (4)$$

Moreover, because $d[A]/dt = 0$ when $[A] = [A]_\infty$, intensities proportional to [A], that is, I_{890} and I_{705} must approach nonzero values

at $t = \infty$, as observed, Fig. 4.

Eqn. (4) has a solution of the form (deleting brackets for concentration),

$$\ln \left[B/ (A - A_\infty)\right] = k_2 B_\infty t + \ln \left[B_o/(A_o - A_\infty)\right], \qquad (5)$$

where $k = A + B = A_o + B_o = A_\infty + B_\infty$ (note that $k \neq K_2$), and rearrangement of eqn. (5) yields the B concentration,

$$B = B_\infty / \left\{1 + \left[(A_o - A_\infty)/B_o\right] \exp(-k_2 B_\infty t)\right\}, \qquad (6)$$

which is seen to be a special case of eqn. (8).

The form of eqn. (6) is convenient for determining the product $k_2 B_\infty$. However, it is necessary to substitute $B_\infty - B$ in the left hand side for $A - A_\infty$ to obtain the intensity ratio $B/(B_\infty - B)$. This substitution allows the intensity ratio for each of the three sets of intensity data to be determined individually. A logarithmic plot of the intensity ratios is shown in Fig. 5 ($\log_{10}\left[B/(B_\infty - B)\right]$ versus t). (For this plot $B = I_i(t)$ for $i = 1556$ cm^{-1}, and $B = I_i(0) - I_i(t)$ for $i = 705$ and 890 cm^{-1}.) Generally good agreement is evident between the three sets of data up to $t = 3$ or 4 h, and this agreement suggests that the data refer to a common process, eqn. (3).

The data of Fig. 5 were treated together by least squares for $0 < t < 3$ h, and the result is shown by the solid line. For $t > 3$ or 4 h considerable deviation of the data from the solid line is apparent.

5

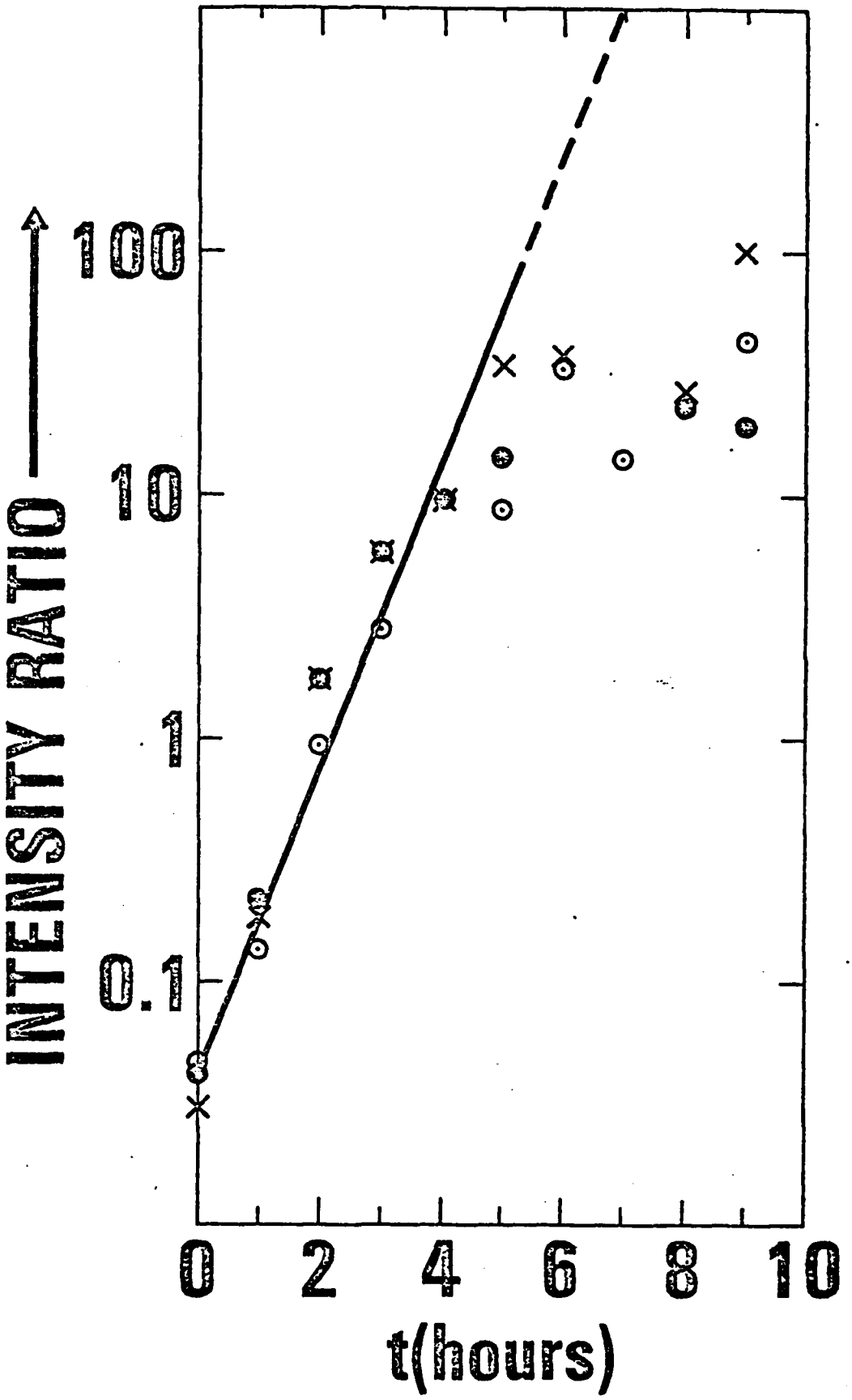

Caption

Figure 5. The intensity ratio $B/(B_{\infty} - B)$ plotted on a logarithmic scale ($\log_{10}$) versus t for heating of EMPB's at 115° C. Solid heavy line refers to least squares fit of the data to 3 h. $B = I_i(t) + k/(1 + C)$ for $i = 1556$ cm^{-1} and $B = I_i(0) - I_i(t) + k/(1 + C)$ for $i = 705$ and 890 cm^{-1}. Filled circles, crosses, and open circles refer, respectively, to 705, 890, and 1556 cm^{-1}.

However, inspection of Fig. 4 clearly indicates that the intensity data do not yield reliable rate information for $t > 3$ or 4 h, and hence the discrepancy is probably not very important.

From the least squares fit, Fig. 5, it is possible to obtain the slope S (in terms of natural logarithms), $S = k_2 B_\infty = 1.6 \pm 0.1\ h^{-1}$. To obtain a value of k_2 in units of liter O_2 $mole^{-1}$ h^{-1} it is necessary to know B_∞. If B_o is considered to be negligible, as observed, the initial concentration ($t = 0$) of peroxy groups, A_o, in mole O_2 $liter^{-1}$, is given by ρ/M, where $M = 99.8$ g, and $\rho = 2.10 \times 10^3$ g $liter^{-1}$.(15) Note that one mole of peroxy O_2 is associated with one mole of Na in $NaBO_2 \cdot H_2O_2$ or $NaBO_3 \cdot H_2O$. Thus, $A_o \tilde{=} 21.0$ mole O_2 $liter^{-1}$. Further, from Raman intensities, Fig. 4, and the assumption that $I_i(t) \propto [\text{peroxy } O_2]$ ($i = 705$ or 890 cm^{-1}), $A_\infty \tilde{=} 8.30$ mole O_2 $liter^{-1}$. Then from $A_o \tilde{=} A_\infty + B_\infty$, $B_\infty = 12.7$ mole O_2 $liter^{-1}$. Therefore, from $k_2 B_\infty = 1.6 \pm 0.1\ h^{-1}$, $k_2 = (1.3 \pm 0.1) \times 10^{-1}$ liter O_2 $mole^{-1}$ (of $NaBO_3 \cdot H_2O$) h^{-1}, at 115° C.

Finally, in regard to mechanisms, the results of Fig. 5 in conjunction with eqns. 3 – 6 imply that the peroxyborate anion decomposes to yield trapped molecular O_2 such that the sum of the peroxy and trapped O_2 concentration is constant. Further, as the concentration of molecular O_2 increases, it increasingly catalyzes the decomposition of the peroxyborate ion. However, as the concentration of molecular O_2 rises, a reverse reaction also occurs that increasingly opposes this rise, such that $I_{705}(\infty)$ or $I_{890}(\infty) \neq 0$.

This, because of mass conservation, means that $I_{1556}(\infty)$ does not rise as high as it would if $I_{705}(\infty)$ or $I_{890}(\infty)$ were zero, i.e., $k - A_\infty$ is smaller for $A_\infty \neq 0$ than for $A_\infty = 0$. A plausible explanation for the reverse reaction is that there is a limit to which the concentration of trapped molecular O_2 can rise because the void volume in the amorphous EMPB is limited. Another feature of the present results is that the molecular O_2 concentration cannot be identically zero at t = 0. Low concentrations of molecular O_2 would be difficult to detect at $0 < t < 1$ h, and further the quantity $\left[k/(1 + C)\right]$ which makes $L_i(0) \equiv 0$ is within the noise level of the 1556 cm^{-1} line. Thus trace amounts of molecular O_2 would seem to be present in the unreacted EMPB to catalyze the initial decomposition of the peroxy groups, or the initial catalysis may also involve paramagnetic species produced by the heating process, e.g., the ESR resonances designated as X, Z, and Y in Ref. (6) which correspond to $BO_3O_2^{\bullet}$, O_2^-, and O_3^-, and whose concentrations are about 10^{21} cm^{-3}, 10^{19} cm^{-3}, and 10^{17} cm^{-3}, resp.(6)

Summary

Raman spectra from a series of EMPB preparations and from Na_2O_2 and BaO_2 were obtained by surface scattering from spinning samples. The data from the heated peroxyborates are consistent with the breakdown of peroxy groups in the peroxyborate anion to form molecular O_2 trapped by the amorphized network. The kinetics of this reaction were treated using quantitative Raman intensity data obtained as a function of heating time at 115° C. Fitting of the data by logistics theory indicates that the breakdown of peroxy groups is auto-catalyzed by the O_2 formed, but that a reverse reaction also involving O_2 limits the reaction at 115° C. However, data at elevated temperatures indicate that most (or all) of the peroxy oxygen can be converted to trapped O_2. For example, at 155° C the forward rate constant, k_2, is apparently much greater than the reverse rate constant, k_1, because $k_2/k_1 = 1/A_\infty$, and A_∞ is very small as evident from low values of I_{705} and I_{890}.

ACKNOWLEDGEMENTS

Numerous helpful discussions with H. D. Ladouceur are gratefully acknowledged. Thanks are also due to S. R. Samanta and M. Hokmabadi for obtaining Raman data, and to M. Krishnamurthy for use of a constant temperature oven. This work was supported by contracts from the Office of Naval Research (laser-Chemistry).

APPENDIX I

According to logistics theory[13] a rate equation of the type,

$$dy/dt = \Phi(t)\, y\, (y-k), \tag{7}$$

has a solution,

$$y = k/\left[1 + Ce^{g(t)}\right], \tag{8}$$

where the function $g(t)$ in equation (8) is given by,

$$g(t) = k \int \Phi(t)\, dt. \tag{9}$$

The simple case where $\Phi(t) = -a/k$ which gives $g(t) = -at$, is found to be sufficiently accurate for the present purposes, and this leads to a solution of the form $y = k/(1 + Ce^{-at})$.

At $t = 0$, the solution y has a finite value, $k/(1 + C)$, while at large t, it has a value k. In Fig. 4(a), it can be seen that the 1556 cm^{-1} intensity is virtually zero at $t = 0$. While a direct fit of the function y to the intensity $I_i(t)$, for $i = 1556\ cm^{-1}$, produces only a small value at $t = o$, comparable to the noise level of the 1556 cm^{-1} intensity, it is convenient to constrain that value to be identically zero by considering, instead of y, the function,

$$L_i(t) = \left[k/(1 + Ce^{-at})\right] - \left[k/(1 + C)\right]. \qquad (10)$$

The excellent least squares fit of eqn. (10) to the 1556 cm^{-1} data is shown by the solid curve in Fig. 4(a). The results of similar fits of $L_i(t)$ to $I_i(0) - I_i(t)$ are shown by the solid curves in Fig. 4(b) for 705 and 890 cm^{-1}. In the latter cases, $I_i(0)$ has values of 1.021 and 1.634 for 705 and 890 cm^{-1}, resp. A direct comparison of the curves $L_i(t)$ is made in Fig. 6, and the least squares values for the parameters a, C, and k are given in the caption for that figure. The favorable comparisons between (a) and (b) in Fig. 6 suggest that molecular O_2 is formed at the expense of peroxy groups in the peroxyborate anion, i.e., the sum of the concentrations of the peroxy groups and molecular O_2 is constant (subsequently described by $k = [A] + [B]$, where A refers to peroxy, and B to O_2).

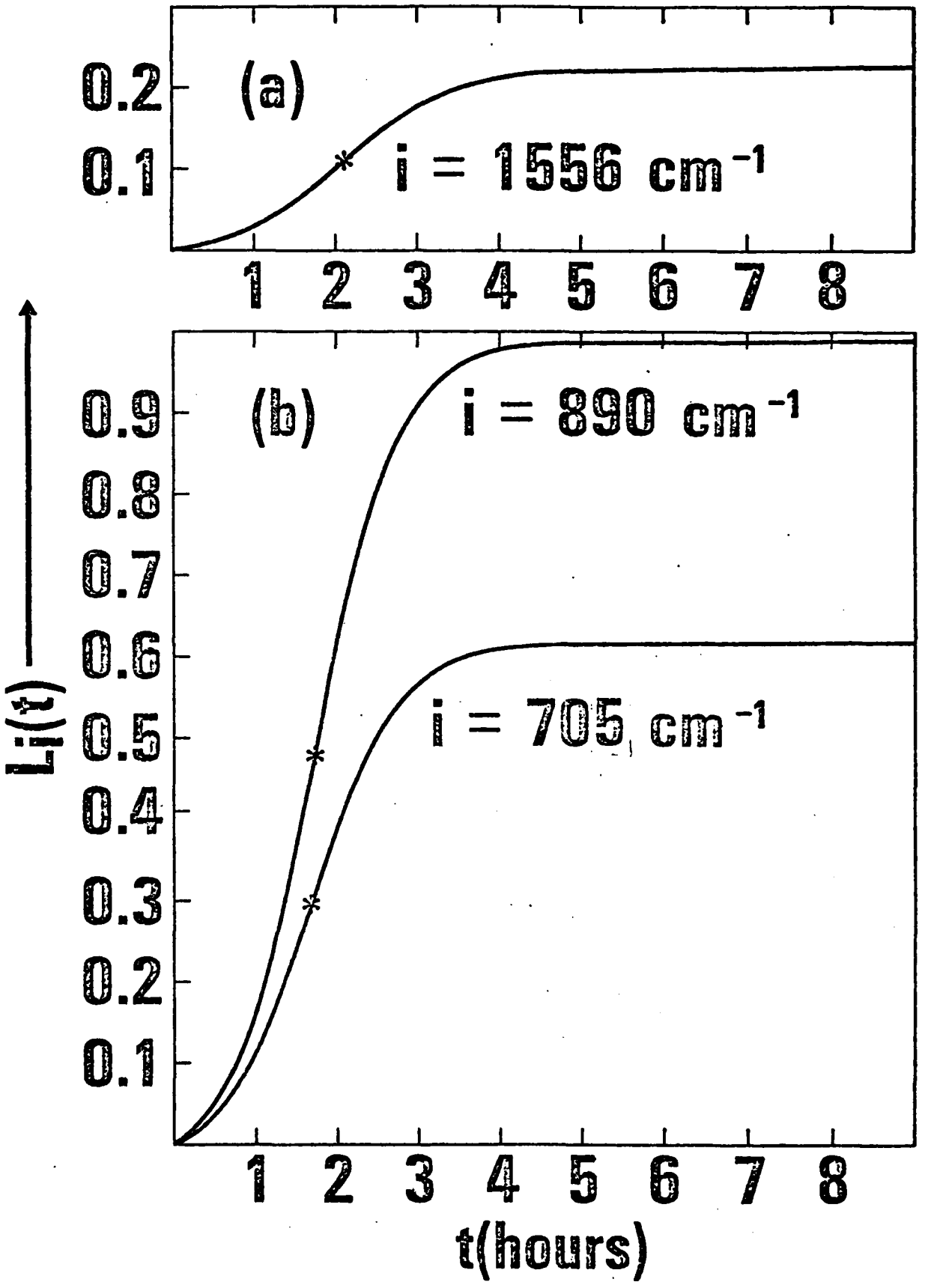
(a)
i = 1556 cm⁻¹
0.2
0.1
1 2 3 4 5 6 7 8
(b)
i = 890 cm⁻¹
i = 705 cm⁻¹
Li(t)
0.9
0.8
0.7
0.6
0.5
0.4
0.3
0.2
0.1
1 2 3 4 5 6 7 8
t(hours)

Caption

Figure 6. Logistics function, $L_i(t)$, as defined in the text used to fit the data shown in Figure 4. The least squares Logistics coefficients are: (1) $i=1556cm^{-1}$; k=0.236 , C=20.8 , a=1.46 ; (2) $i=890\ cm^{-1}$; k=1.02 , C=28.8 , a=1.94 ; and (3) $i=705cm^{-1}$; k=0.646 , C=22.0 , and k=1.86 . The stars shown on the three curves refer to inflection points corresponding to (k/2) - [k/(1+C)].

Visual inspection of the curves shown in Figs. 4 and 6 indicates inflections near 1.5 - 2.0 h in all cases. More accurate positions can be determined using logistics theory from which inflections occur when $\Phi'(t) + \Phi^2(t)(2y-k) = 0$, where the prime denotes differentiation with respect to t. Hence, when $\Phi(t) = -a/k$, the inflection must occur at $y = k/2$. However, when $L_i(t)$ is used, the corresponding inflection occurs at $L_i(t) = (k/2) - \left[k/(1 + C)\right]$. Accordingly, in Fig. 6 the inflections occur at $L_{1556}(t) = 0.1071$, at $L_{890}(t) = 0.4772$, and at $L_{705}(t) = 0.2948$. The corresponding times in Fig. 6 are 2.1 h for (a) and 1.75 h and 1.70 h for (b). These times refer to maxima in the corresponding derivatives dI_i/dt, and hence to the times when the rate of change of the peroxy and molecular O_2 concentrations are maximal. The range 1.70-1.75 h is considered to be a more accurate estimate than the value of 2.1 h, however, because the 1556 cm^{-1} intensity that leads to the 2.1 h value is subject to larger errors.

APPENDIX II

It is known that the O-O stretching frequency generally increases as electrons are removed, cf., O_2^{2-}, 728-844 cm^{-1}, this work; O_2^-, 1136 cm^{-1}, this work, or 1145 cm^{-1}(11); O_2, 1556 cm^{-1}(10); and, O_2^+, 1876 cm^{-1}(16). Similarly, the principal Raman frequency from Na_2O_2 occurs at 738 cm^{-1}, whereas that from the presumably less negative peroxide ion in BaO_2 occurs at 844 cm^{-1}. Also, O-O stretching occurs at 877 cm^{-1} for H_2O_2;(16) and between 890-945 cm^{-1} for some covalent organic peroxides.(17) Hence, it is reasonable to assign the intense line at 890 cm^{-1} to peroxy stretching in the peroxyborate anion, but it seems unreasonable to assign the 705 cm^{-1} line to an ionic peroxy group, as might be required by the above comparisons.

The present Raman data indicate that the 705 and 890 cm^{-1} intensities scale quantitatively together, Figs. 4 and 6, and examinations of Raman spectra obtained between 110° C and 180° C indicate that the 960 cm^{-1} intensity, Fig. 2, also scales qualitatively with the 705 and 890 cm^{-1} intensities. However, because there are only two peroxy bonds in the peroxyborate anion, no more than two peroxy valence vibrations, i.e., stretching along the double bond direction, can be expected. These two valence vibrations would be degenerate if the intraionic coupling is weak, but if the coupling is strong, the in-phase valence mode would be intense in the Raman spectrum, with the out-of-phase valence mode weak, (or vice versa for the infrared spectrum). Hence, one strong

APPENDIX

peroxy stretching line would be expected in the Raman spectrum, rather than two or three, and it would be most likely to occur at 890 cm^{-1}. Accordingly, the 705 and 960 cm^{-1} lines probably arise from other vibrations, and if they arise from the $B_2(O_2)_2$ ring of the peroxyborate anion, their intensities would probably scale with the 890 cm^{-1} peroxy intensity because all three modes would be associated solely with unbroken $B_2(O_2)_2$ units. However, the totally symmetric stretching and asymmetric stretching vibrations of the tetrahedral $B(OH)_4^-$ ion occur at 747-754 cm^{-1} and 945-950 cm^{-1}, respectively,[18] and the symmetric B-OH stretching of H_3BO_3 occurs at 1060 cm^{-1}.[18] Thus the possibility that the 705 and 960 cm^{-1} lines are related to $B-OH^-$ or B-OH groups of the peroxyborate ion cannot be ruled out.

Finally, infrared spectra were not obtained in this work. However, several spectra have been reported for $NaBO_3 \cdot H_2O$, see for example Ref. (19).

REFERENCES

1. Peroxyborates are also called perborates. However, the term metaborate refers to salts formally containing the BO_2^- ion, e.g., $NaBO_2$.
2. The formulas $NaBO_3 \cdot H_2O$ or $NaBO_2 \cdot H_2O_2$ and $NaBO_3 \cdot 4H_2O$ or $NaBO_2 \cdot H_2O_2 \cdot 3H_2O$ refer primarily to stoichiometry, but they might also be written as $Na_2[B_2(O_2)_2(OH)_4]$ and $Na_2[B_2(O_2)_2(OH)_4] \cdot 6H_2O$, respectively, where $[B_2(O_2)_2(OH)_4]^{2-}$ is the peroxyborate anion. Note that $NaBO_3 \cdot H_2O$ is actually not a hydrate, whereas $NaBO_3 \cdot 4H_2O$ or $NaBO_2 \cdot H_2O_2 \cdot 3H_2O$ is a true hydrate.
3. A. Hansson, Acta Chem. Scand. 15, 934(1961).
4. R. Bruce, J. O. Edwards, D. L. Griscom, R. A. Weeks, L. R. Darbee, W. DeKleine, and M. McCarthy, J. Am. Chem. Soc. 87, 2057(1965).
5. J. O. Edwards, D. L. Griscom, R. B. Jones, K. L. Watters, and R. A. Weeks, J. Am. Chem. Soc. 91, 1095(1969).
6. D. L. Griscom, Ph. D. dissertation, Brown Univ., 1966.
7. H. Meyer, M. C. O'Brien, and J. H. Van Vleck, Proc. Roy. Soc. (London) A243, 414(1958).
8. E. G. Brame,Jr., S. Cohen, J. L. Margrave, and V. W. Meloche, J. Inorg. Nucl. Chem. 4,90(1957).
9. The specific sample spinning method used here was described by G. E. Walrafen and S. R. Samanta, Appl. Spectrosc. 33, 524(1979).
10. A. Weber and E. A. McGinnis, J. Mol. Spectry. 4, 195(1960).
11. J. A. Creighton and E. R. Lippincott, J. Chem. Phys. 40, 1779(1964

REFERENCES

12. Electron irradiated samples were examined here because they were available from the work of Ref. (6).

13. H. T. Davis, "Introduction to Nonlinear Differential and Integral Equations," Dover, New York, 1960.

14. J. W. Moore and R. G. Pearson, "Kinetics and Mechanisms," Wiley, New York, 1981.

15. "FMC, Sodium Perborate, Tetrahydrate/Monohydrate," Product Information Bulletin, FMC Corporation, 2000 Market St., Philadelphia, Pa. 19103.

16. G. Herzberg, "Infrared and Raman Spectra of Polyatomic Molecules," Wiley, New York, 1945.

17. E. Maslowsky, Jr., "Vibrational Spectra of Organometallic Compounds," Wiley, New York, 1977, pgs. 123, 422.

18. K. Nakamoto, "Infrared Spectra of Inorganic and Coordination Compounds," Wiley, New York, 1963, pgs. 90 and 107.

19 Coblentz Spectra, No. 2382, Sadtler Research Labs., Philadelphia, Pa. 19104. R. A. Nyquist and R. O. Kagel, "Infrared Spectra of Inorganic Compounds," Academic Press, New York, 1971.

TECHNICAL REPORT DISTRIBUTION LIST, GEN

	No. Copies
Office of Naval Research Attn: Code 472 800 North Quincy Street Arlington, Virginia 22217	2
ONR Branch Office Attn: Dr. George Sandoz 536 S. Clark Street Chicago, Illinois 60605	1
ONR Area Office Attn: Scientific Dept. 715 Broadway New York, New York 10003	1
ONR Western Regional Office 1030 East Green Street Pasadena, California 91106	1
ONR Eastern/Central Regional Office Attn: Dr. L. H. Peebles Building 114, Section D 666 Summer Street Boston, Massachusetts 02210	1
Director, Naval Research Laboratory Attn: Code 6100 Washington, D.C. 20390	1
The Assistant Secretary of the Navy (RE&S) Department of the Navy Room 4E736, Pentagon Washington, D.C. 20350	1
Commander, Naval Air Systems Command Attn: Code 310C (H. Rosenwasser) Department of the Navy Washington, D.C. 20360	1
Defense Technical Information Center Building 5, Cameron Station Alexandria, Virginia 22314	2
Dr. Fred Saalfeld Chemistry Division, Code 6100 Naval Research Laboratory Washington, D.C. 20375	1
U.S. Army Research Office Attn: CRD-AA-IP P.O. Box 1211 Research Triangle Park, N.C. 27709	1
Naval Ocean Systems Center Attn: Mr. Joe McCartney San Diego, California 92152	1
Naval Weapons Center Attn: Dr. A. B. Amster, Chemistry Division China Lake, California 93555	1
Naval Civil Engineering Laboratory Attn: Dr. R. W. Drisko Port Hueneme, California 93401	1
Department of Physics & Chemistry Naval Postgraduate School Monterey, California 93940	1
Dr. A. L. Slafkosky Scientific Advisor Commandant of the Marine Corps (Code RD-1) Washington, D.C. 20380	1
Office of Naval Research Attn: Dr. Richard S. Miller 800 N. Quincy Street Arlington, Virginia 22217	1
Naval Ship Research and Development Center Attn: Dr. G. Bosmajian, Applied Chemistry Division Annapolis, Maryland 21401	1
Naval Ocean Systems Center Attn: Dr. S. Yamamoto, Marine Sciences Division San Diego, California 91232	1
Mr. John Boyle Materials Branch Naval Ship Engineering Center Philadelphia, Pennsylvania 19112	1

TECHNICAL REPORT DISTRIBUTION LIST, 051A

	No. Copies
Dr. M.A. El-Sayed Department of Chemistry University of California, Los Angeles Los Angeles, California 90024	1
Dr. E. R. Bernstein Department of Chemistry Colorado State University Fort Collins, Colorado 80521	1
Dr. C. A. Heller Naval Weapons Center Code 6059 China Lake, California 93555	1
Dr. J. R. MacDonald Chemistry Division Naval Research Laboratory Code 6110 Washington, D.C. 20375	1
Dr. G. B. Schuster Chemistry Department University of Illinois Urbana, Illinois 61801	1
Dr. A. Adamson Department of Chemistry University of Southern California Los Angeles, California 90007	1
Dr. M. S. Wrighton Department of Chemistry Massachusetts Institute of Technology Cambridge, Massachusetts 02139	1
Dr. M. Rauhut Chemical Research Division American Cyanamid Company Bound Brook, New Jersey 08805	1
Dr. J. I. Zink Department of Chemistry University of California, Los Angeles Los Angeles, California 90024	1
Dr. D. Haarer IBM San Jose Research Center 5600 Cottle Road San Jose, California 95143	1
Dr. John Cooper Code 6130 Naval Research Laboratory Washington, D.C. 20375	1
Dr. William M. Jackson Department of Chemistry Howard University Washington, DC 20059	1
Dr. George E. Walraffen Department of Chemistry Howard University Washington, DC 20059	1

	No. Copies
Dr. Rudolph J. Marcus Office of Naval Research Scientific Liaison Group American Embassy APO San Francisco 96503	1
Mr. James Kelley DTNSRDC Code 2803 Annapolis, Maryland 21402	1